PCCP

Accepted Manuscript

ROYAL SOCIETY OF CHEMISTRY

www.rsc.org/pccp

Electronic Storage Capacity of Ceria: Role of Peroxide in Au_x Supported on CeO_2 (111) Facet and CO Adsorption

Yinli Liu,[a] Huiying Li,[a] Jun Yu,[a] Dongsen Mao,[a] and Guanzhong Lu*[a,b]*

[a] Research Institute of Applied Catalysis, Shanghai Institute of Technology, 100 Haiquan Road, Shanghai 201418, P. R. China

[b] Key Laboratory for Advanced Materials and Research Institute of Industrial catalysis, East China University of Science and Technology, 130 Meilong Road, Shanghai 200237, P. R. China

***Corresponding Authors:** Fax: +86-21-60879111. E-mail: gzhlu@ecust.edu.cn (G.Z. Lu);

Fax: +86-21-60877231. hyli@sit.edu.cn (H.Y. Li).

Abstract: The density functional theory (DFT+U) was used to study the adsorption of Au_x (x=1-4) clusters on the defective CeO_2(111) facet and CO adsorption on the corresponding Au_x/CeO_{2-x} catalyst, in which much of the work is CeO_{2-x} + superoxide/peroxide then Au_x is added. When Au_1 supported on the CeO_2(111) facet with an O vacancy, the strong electronegative $Au^{\delta-}$ formed is not favorable for CO adsorption. When peroxide adsorbed on the CeO_2(111) facet with the O vacancy, Au_x was oxidized, resulting in stable Au_x adsorption on the defective ceria surface with peroxide, which promotes CO adsorption on the Au_x/CeO_{2-x} catalyst. With more Au atoms in supported Au_x clusters, CO adsorption on this surface becomes stronger. During both Au supported on CeO_{2-x} and CO adsorbed on Au_x/CeO_{2-x}, CeO_2 acts as an electron buffer that can store/release the electrons. These results provide a scientific understanding for the development of high-performance rare earth catalytic materials.

Keyword: DFT+U, Au/CeO_2 catalyst; Oxygen vacancy; Adsorbed peroxide; CO adsorption.

1. Introduction

Ceria supported gold (Au/CeO_2) catalysts have become one of the hottest systems in catalysis, being widely applied to many important processes, such as CO oxidation,[1–3,] water-gas shift (WGS) reaction,[4–7,] methanol synthesis,[8] hydrocarbon oxidation,[9] and NO reduction,[10–12] and automotive exhaust purification.[13]

Since the pioneering work (Au/oxides) of Haruta,[14] ceria supported gold catalysts and its role in CO oxidation has been drawing extensive interest experimentally and theoretically. Contributions from literatures can be summarized in three major aspects: (i) The size-dependent catalytic activity of supported Au catalysts has been extensively studied, and supported gold clusters of size smaller than 5 nm exhibit very high surface reactivity.[15–21] (ii) $Au^{\delta+}$ species stabilized on oxide can act as active sites, while $Au^{\delta-}$ ions are inactive for CO adsorption.[22,23] The experimental results are consistent with theoretical research results.[1,6,24,25] Those studies reveal that oxygen vacancies increase the adsorption or binding of Au on the ceria surface.[4,26,27] However, an interaction of Au with oxygen vacancy tends to form negatively charged Au,[24,28] which is inactive for CO adsorption. Thus, how to transfer the charge from Au cluster to some other species so that the Au will be active for CO interaction is an important topic. (iii) The role of ceria.[29–31] Nanocrystalline CeO_2 support can enhance the activity of Au for CO oxidation,[29] and the reactive oxygen on nano Au/CeO_2 crystallite surface exists in the form of superoxide (O_2^-) and peroxide (O_2^{2-}) ad-species during CO oxidation at low temperature.[23,32] In an oxygen atmosphere, superoxide and peroxide are two kinds of important oxygen species on the CeO_2 (111) surface, which can be characterized by electron paramagnetic resonance (EPR), Raman and FT-IR spectroscopies.[23,33–37] We found that on the reduced CeO_2 (111) facet, oxygen adsorbed on a surface vacancy forms a peroxide, and oxygen adsorbed on a subsurface vacancy forms a superoxide by the density functional theory (DFT+U) calculations.[38] Fabris and Huang studied the adsorption behaviors of superoxide on the CeO_2 (111) with O vacancy and CeO_2 (110) facets.[39] Using DFT+U approach, Teng *et al*. investigated the electronic properties of superoxide and peroxide species on a partially reduced

CeO_2 (111) model catalyst.[40] They also found that CO can be directly oxidized to CO_2 by the superoxide without an energy barrier, while carbonate can form when CO reacts with peroxide. After O_2 adsorbed on Au_3/CeO_2 (110) surface, we found, O_2^- species could form.[41]

Theoretical study with DFT+U method is a powerful tool to understand the catalysis or catalytic reaction mechanism, and can be adopted to study the vacancy, metal doping, and adsorption/reaction mechanism on the ceria catalyst.[42–51] Although theoretical studies of Au/CeO_2 as above-mentioned provide plenty information, there are still two major basic challenges to be identified with more insights: (1) how to make gold clusters adhere well on the ceria surface; (2) what is the role of Ce *f*-orbit during Au adsorption on ceria and CO adsorption over the surface of Au/ceria. Therefore, using DFT+U methods, we studied in detail the influence of O vacancy, peroxide and superoxide species on the gold adsorption on ceria and CO adsorption on the resulting $Au/CeO_2(111)$ structure. We try to provide deeper insights into the origin of Au_x clusters adsorption on the CeO_2 surface, the electrons transfer mechanism and how CeO_2 acts as an electron buffer.

This work is organized as follows. The calculation details are mentioned in section 2. The interactions of Au_x clusters with O vacancy, peroxide and superoxide on the CeO_2 (111) facet are studied in section 3, including the CO adsorption on the surface. Finally, the conclusions are summarized in section 4. The results show that, the adsorbed peroxide can promote the adsorption of Au_x on ceria and CO adsorption on Au_x/CeO_{2-x} catalyst, and CeO_2 acts as an electron buffer during the adsorption process.

2. Computational details

The calculations were carried out within the generalized gradient approximation with the VASP.[52,53] The project-augmented wave (PAW) method[54,55] was used to represent the core-valence interaction. The valence electronic states were expanded in plane-wave basis sets with an energy cut-off at 500 eV. The density functional theory (DFT+U) method [50,51,56] was used to treat the highly localized Ce 4f state. The value of U = 5.0 eV was adopted in this work, which is the same

value as most of the literature of Au/CeO_2 system.[57–64]

Being different from the works of Branda *et al*.,[49,50] the ceria surfaces were modeled by a *p*(3×4) unit cell with three CeO_2 layers and the vacuum between slabs was 14 Å. The bottom CeO_2 layers was fixed and all others atoms are relaxed, in which the force threshold was set to 0.02 eV/Å. Monkhorst Pack mesh of (1×1×1) was used for the *k*-point sampling.

In the optimization process, adsorption energies were measured by the following formula, $E_{ads}= -(E_{tot}–E_{sub}–E_x)$, where E_{tot} is the total energy of the combined system, E_{sub} is the energy of the substrate alone, and E_x is the total energy of the adsorbates in the gas phase.

In this work, the Bader charge analysis was utilized for better understanding electron transfer mechanism of Au_x clusters after being supported on the CeO_2 surface. Like the adsorption energy equation, the difference charge density has been evaluated with the expression: $\Delta\rho(r) =\rho_{tot}(r) -\rho_{sub}(r) -\rho_x(r)$, where $\rho_{tot}(r)$, $\rho_{sub}(r)$ and $\rho_x(r)$ are the charge densities of the whole system, isolated substrate, and adsorbate, respectively.

3. Results and discussion

Herein, we first studied a single Au atom adsorption on CeO_2 (111) facet containing oxygen vacancy, peroxide and superoxide, and CO adsorption on Au_1/CeO_2 (111) facet. Structure, charge density difference, adsorption energy as well as the Bader charge were discussed in detail to understand the electron transfer mechanism during either Au absorption on the CeO_2 surface and CO adsorption on the Au_1/CeO_2 (111) surface. Then, we extended this study to Au clusters, i.e. Au_x (x = 2–4), to gain further insights with more practical catalyst and catalysis. The various structures of Au adsorption on the CeO_2 surface were defined as Au_x-$(PO_2)_y$-$(SO_2)_z$-V_m-$(SV)_n$, where PO_2, SO_2, V and SV represent peroxide, superoxide, surface oxygen vacancies and sub-surface oxygen vacancies respectively, and y, z, m and n are the numbers of them.

3.1. Au_1 adsorption on CeO_2 (111) facet and CO adsorption on Au_1/CeO_2

The single Au atom adsorbed at the top site of surface oxygen on the clean CeO_2 (111) facet (Au_1-O-t) was shown in Figure 1a. The Au-O bond length and the calculated adsorption energy are

1.99 Å and 0.98 eV (Table 1) respectively, which aligns well with the reported results (2.00 Å and 1.04 eV, respectively).[24] This result indicates a weak adsorption of single Au atom on the clean CeO_2. A positively charged $Au^{\delta+}$ adatom and a reduced Ce^{3+} ion were found via the charge density difference of Au_1-O-t (Figure 1b). The positively charged $Au^{\delta+}$ was further validated by computing the Bader charge (+0.28e, Table 1). Based on these results, we may explain this adsorption process as below: oxygen on the CeO_2 surface oxidizes Au to form the Au-O bond, thus the electron transfers from neutral Au atom to the Ce surface by Au-O bond, forming Ce^{3+}. This process can be simply described as follows:[65] $Au - e \rightarrow Au^{\delta+}$, $Ce^{4+} + e \rightarrow Ce^{3+}$.

Although the Au_1 adsorption here is weak and no practical meaning, we would like to study further CO adsorption on this positively charged Au (that is the Au_1-O-t surface). As shown in Figure 1c, the C-O bond length is 1.15 Å, and the distance between the C atom and the Au is 1.88 Å. The charge density difference (Figure 1d) shows that Ce^{3+} ion is not changed and the charge of Au is still positive. As shown in Bader charge analysis of Table 1, the charge of $Au^{\delta+}$ is increased from +0.28e to +0.51e after CO adsorption and CO Bader charge is −0.09e, indicating an electron transferred further from the Au atom to CO. Based on this positive charge of Au, the calculated CO adsorption energy is 2.52 eV (Table 1), that is, a strong adsorption.

It was reported that, oxygen vacancy can stabilize Au_x clusters on the reduced CeO_2 (111) facet,[6,24] which is our next interest besides clean surface. The structure or spin density of CeO_2 (111) facet containing single O vacancy is shown Figure S1, two excess electrons are localized at two Ce ions, which is consistent with our previous calculation.[38] As seen in Figure 1e for the adsorption of Au_1 on CeO_2 (111) facet with one oxygen vacancy (Au_1-V_1), Au_1 atom anchored on the oxygen vacancy with a distance of 0.61 Å, and three Au-Ce bonds are 3.16, 3.16 and 3.21Å, respectively. And the corresponding adsorption energy is 2.32 eV (Table 1), which is much stronger than Au_1 on the clean CeO_2 (111) facet. This agrees well with reported results.[66,67] By the help of the charge density difference analysis for the optimized structure (Figure 1f), we found the presence of an $Au^{\delta-}$ adatom and one Ce^{3+} for the (Au_1-V_1) case. It was reported show that, [24,

[38,55,68,69] two Ce^{3+} ions will be generated after formation of one oxygen vacancy. These results indicates an electron transfers from the reduced oxide surface (one of the two Ce^{3+} ions) to the supported Au atom, thus there exists just one Ce^{3+} ion leaving on the reduced surface. The Bader charges in Table 1 show that, the charge of Au is –0.62e, showing a very strong electronegativity. Therefore, CO molecule cannot bind with the $Au^{\delta-}$ species, that is, CO cannot adsorb on the $Au^{\delta-}$ species.[24]

The results above show that, Au_1 adsorption on the reduced surface of CeO_{2-x} with oxygen vacancy is much stronger than on the clean surface of CeO_2 without oxygen vacancy, while an electron transfers from one of two Ce^{3+} ions to Au, resulting in a very strong electronegativity of Au and CO non-adsorption on this $Au^{\delta-}$ species.

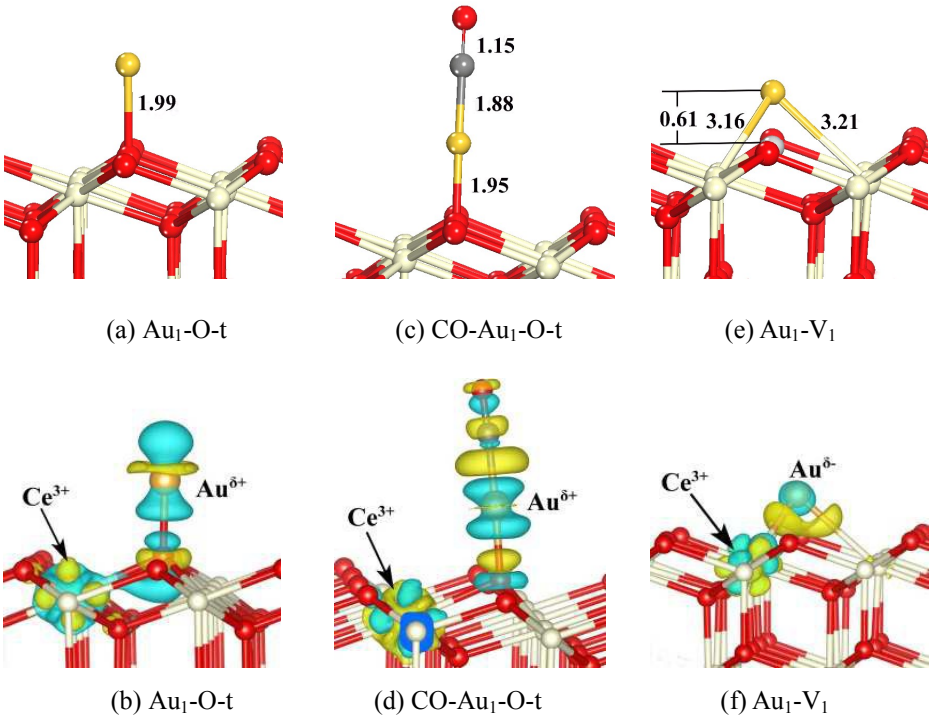

(a) Au_1-O-t (c) CO-Au_1-O-t (e) Au_1-V_1

(b) Au_1-O-t (d) CO-Au_1-O-t (f) Au_1-V_1

Figure 1. Optimized structures of (a, e) Au_1 atom on the CeO_2(111) facet and (c) CO adsorption on Au_1/CeO_2(111), and (b, d, f) the corresponding charge density difference. (O, Ce, Au, C atoms are denoted in red, gray, yellow and dark gray, respectively. The O vacancy is represented by balls in light gray. Main bond lengths are reported in Å. Electron accumulation and depletion are represented by yellow and blue areas, respectively. The isosurface value is set as 0.005 e/Å^3).

To explain the influence of peroxide and superoxide on the Au adsorption, we studied the

adsorption of Au_1 around these oxygen species on the CeO_2 (111) facet.

For one peroxide on the CeO_2 (111) facet, the Au atom bonds with two O atoms with bond lengths of 2.07 Å ($Au\text{-}O_{lattice}$) and 2.09Å ($Au\text{-}O_{peroxide}$), as shown in Figure 2a. The O-O distance within peroxide on the adsorbed surface is 1.49 Å bigger than 1.44 Å of the original distance (Figure S2). The corresponding Au atom adsorption energy is 1.75 eV (Table 1). An $Au^{\delta+}$ and one Ce^{3+} appeared as studied by the charge density difference of this configuration (Figure 2b), and the charge of $Au^{\delta+}$ is +0.34e by the Bader charge calculation (Table 1).

Based on this structure, CO adsorption on its surface was studied. The optimized structure for CO adsorption on this positively charged $Au^{\delta+}$ ion (that is the $Au_1\text{-}(PO_2)_1$ surface) is shown in Figure 2c, and its adsorption energy was calculated to be 1.63eV (Table 1). The C-O bond length of adsorbed CO molecule is 1.15Å, and the distance between the C atom and Au is 1.87 Å, while the Au-O bonds is changed to 2.01 Å ($Au\text{-}O_{lattice}$) and 3.06 Å ($Au\text{-}O_{peroxide}$). As shown from the charge density difference in Figure 2b and 2d, one Ce^{3+} ion exists before and after CO adsorption, and the Bader charge analysis shows Au has a positive charge +0.51e (Table 1). This shows the charge transfers from $Au^{\delta+}$ adatom to the CO at the Au/CO interface, where the adsorbed $Au^{\delta+}$ ion can act as an active site for CO adsorption on the CeO_2 (111) surface with a peroxide.

Au_1 adsorption on the CeO_2(111) facet containing a subsurface O vacancy and a superoxide ($Au_1\text{-}(SO_2)_1\text{-}(SV)_1$) is shown in Figure 2e. The $Au\text{-}O_{superoxide}$ bond length is 2.08 Å and the O-O bond within superoxide is elongated to 1.38 Å from 1.33 Å (Figure S2). As shown in the charge density difference analysis of $Au_1\text{-}(SO_2)_1\text{-}(SV)_1$ (Figure 2f), there is an $Au^{\delta+}$ ion and Ce^{3+}. The reduced Ce^{3+} ion is resulted from the subsurface O vacancy. Furthermore, the Au-*d* band and the O-2*p* band of the superoxide are overlapped. The Bader charge analysis shows that Au has positive charge +0.17e (Table 1), that is, an electron transfers from Au atom to superoxide, forming positively charged $Au^{\delta+}$. The Au_1 adsorption energy was calculated to be 1.08 eV, which is less than Au_1 on the CeO_2 (111) surface with a peroxide (1.75 eV). When CO adsorbed on this surface ($Au_1\text{-}(SO_2)_1\text{-}(SV)_1$), the superoxide structure would rearrange to form the structure with a peroxide

($CO\text{-}Au_1\text{-}(PO_2)_1$, Figure 2c), because of the instability of superoxide.[40] The structure rearrangement includes two parts: (1) when CO is close to Au_1, because of the structure effect, the surface oxygen O_A migrates to the subsurface vacancy position, forming the subsurface oxygen and a surface vacancy; (2) once the new surface oxygen vacancy is formed, the nearby oxygen O_B of superoxide would easily migrate to the surface vacancy to form peroxide. The CO adsorption energy is 3.19 eV, which may include both CO adsorption energy and structure rearrangement energy. The structure rearrangement energy includes two parts: (1) migration energy from surface oxygen to subsurface oxygen ($O_V \rightarrow O_{SV}$), and (2) migration energy from superoxide to peroxide. In summary, for the $CeO_2\text{-}(SO_2)_1\text{-}(SV)_1$ sample, Au_1 adsorption on its surface is not stable enough comparing with that on its structure with peroxide, because during CO adsorption, its structure was rearranged back to the structure with a peroxide ($CO\text{-}Au_1\text{-}(PO_2)_1$). Hence in the following discussions, we will take major focus on the structure with a peroxide ($CeO_2\text{-}(PO_2)_1$).

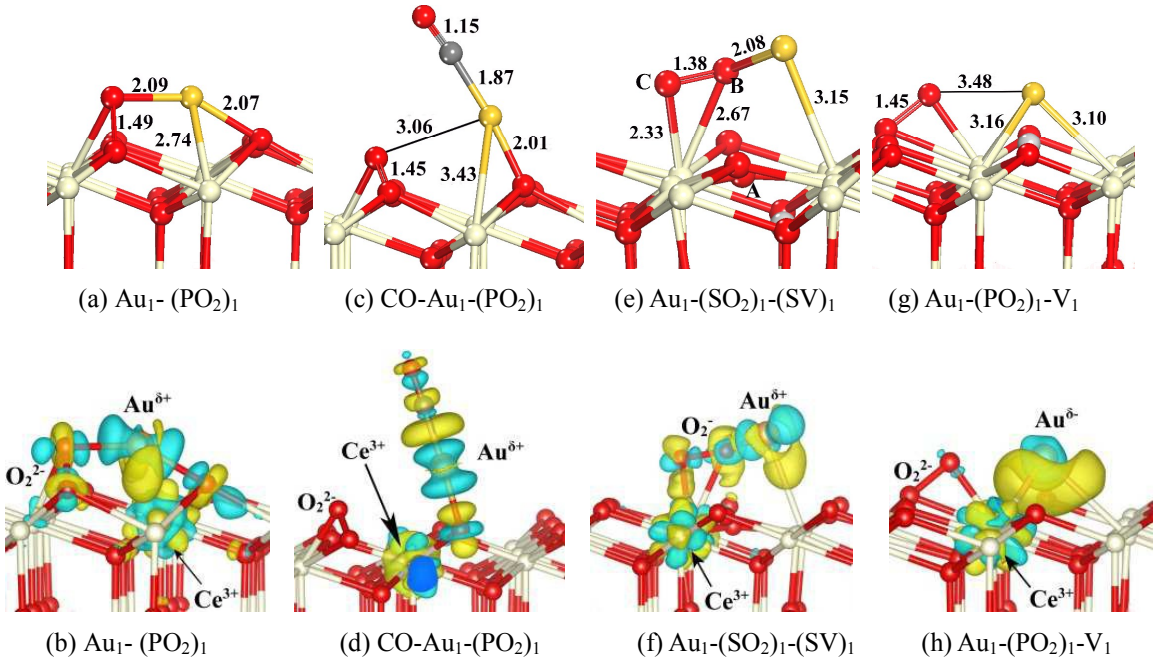

(a) $Au_1\text{-}(PO_2)_1$ (c) $CO\text{-}Au_1\text{-}(PO_2)_1$ (e) $Au_1\text{-}(SO_2)_1\text{-}(SV)_1$ (g) $Au_1\text{-}(PO_2)_1\text{-}V_1$

(b) $Au_1\text{-}(PO_2)_1$ (d) $CO\text{-}Au_1\text{-}(PO_2)_1$ (f) $Au_1\text{-}(SO_2)_1\text{-}(SV)_1$ (h) $Au_1\text{-}(PO_2)_1\text{-}V_1$

Figure 2. Optimized structures of (a, e, g) Au_1 atom on the $CeO_2(111)$ facet and (c) CO adsorption on $Au_1/CeO_2(111)$, and (b, d, f, h) the corresponding charge density difference. (O, Ce, Au, C atoms are denoted in red, gray, yellow and dark gray, respectively. The O vacancy is represented by balls in light gray. Main bond lengths are reported in Å. Electron accumulation and depletion are represented by yellow and blue areas, respectively. The isosurface value is set as 0.005 e/Å^3).

Those results above suggest that the presence of vacancy, peroxide and superoxide helps to the adsorption of Au_1 on the CeO_2(111) facet, compared with the clean CeO_2 (111) facet, and their corresponding adsorption energy are 2.30 eV, 1.75 eV, 1.08 eV and 0.98 eV, respectively. While none of these adsorption currently can overcome Au-Au binding (binding energy is 2.31eV based on formula $E_{Au-Au}=E(Au)_2-2E_{Au}$). Thus there is a question: if the CeO_2 (111) facet has the peroxide and O vacancy simultaneously, that is, CeO_2-$(PO_2)_y$-V_m, can it help to the Au adsorption?

Table 1. The Au_1 or CO adsorption energy (eV) and the Bader charge of Au_1 clusters and CO

	E_{ad} /eV	Au-Bader charge /e	CO-Bader charge /e
Au_1-O-t	0.98	+0.28	
CO-Au_1-O-t	2.52	+0.51	-0.09
Au_1-V	2.30	-0.62	
Au_1-$(PO_2)_1$	1.75	+0.34	
CO-Au_1- $(PO_2)_1$	1.63	+0.51	-0.05
Au_1-$(SO_2)_1$- $(SV)_1$	1.08	+0.17	
Au_1- $(PO_2)_1$-V_1	2.32	-0.60	

The calculated structure and charge density difference for CeO_2-$(PO_2)_1$-V_1 are shown in Figure S2, and the calculated structure for Au_1-$(PO_2)_1$-V_1 is shown in Figure 2g. The distance between Au atom and $O_{peroxide}$ reaches ~3.48 Å, and there is no electron interaction between them. The Au_1 adsorption energy is 2.32 eV in this configuration, which is same as Au-Au binding energy (2.31eV). This suggests that, when peroxide and oxygen vacancies exist simultaneously on the CeO_2 surface, it is advantageous to the adsorption of gold clusters and inhibits it reunion on the CeO_2 (111) facet. That is to say, when the adsorbed Au migrates from CeO_2 (111) facet toward Au-Au reunion, it should overcome the adsorption energy, i.e., a minimum 2.32 eV, thus this process carries on difficultly.

The charge density difference analysis of this structure displayed $Au^{\delta-}$ and one Ce^{3+} ion on the surface (Figure 2h), and the charge transferred from the surface of reduced oxide Ce^{3+} to the Au atom, thus resulting in a negatively charged $Au^{\delta-}$ adatom presented on the surface. The Bader

charge analysis shows that the charge of the adsorbed Au is −0.60e. Hence CO molecule cannot adsorb on its surface, or say, CO cannot bind with $Au^{\delta-}$.

For single Au atom adsorption on the CeO_2 (111) facet, we have found that, firstly, the stability of a single Au atom adsorption is changed in following order of $(PO_2)_1$-V_1> V_1 > $(PO_2)_1$ > $(SO_2)_1$-$(SV)_1$> clean CeO_2(111) facet, where the combination of peroxide and O vacancy provides the best surface for Au adsorption (even slightly better than Au-Au binding). Secondly, CO could adsorb easily at the positively charged $Au^{\delta+}$. In this way, even the most promising structure, $(PO_2)_1$-V_1, because of the strongly negatively charged $Au^{\delta-}$, CO molecule cannot adsorb on its surface. Lastly, after Au adsorption on CeO_2 (111) facet with one peroxide, a reduced Ce^{3+} is presented. And ceria has a capacity for storing electrons. In the following study on two Au atoms (Au_2), we will continually explore the situation of peroxide adsorbed on the CeO_2 (111) facet with and without O vacancy.

3.2. Au_2 cluster adsorbed on the CeO_2 (111) surface and CO adsorption

The optimized structures of Au_2 clusters on reduced CeO_2 (111) facets (containing two peroxide or both one oxygen vacancy and two peroxide) and CO adsorption on the Au_2/CeO_2 catalyst, and their charge density difference analyses are shown in Figure 3. The corresponding adsorption energies and Bader charge data of Au_2 cluster are listed in Table 2.

Table 2. The Au_2 cluster or CO adsorption energy (eV) and the Bader charge of Au_2 clusters

	E_{ad} /eV	Au-Bader charge /e		CO-Bader charge /e
		Au_A	Au_B	
Au_2-$(PO_2)_2$	1.16	+0.07	+0.05	
CO-Au_2-$(PO_2)_2$	1.20	+0.17	-0.13	-0.05
Au_2-$(PO_2)_2$-V_1-L	2.65	-0.05	-0.12	
CO-Au_2-$(PO_2)_2$-V_1-L	0.51	+0.10	-0.16	-0.02

As shown in Figure 3a, for the CeO_2 (111) facet with two peroxide, Au_2 lies parallel on the surface (Au_2-$(PO_2)_2$). The two gold atoms are anchored by two peroxides, two bond lengths of Au-$O_{peroxide}$ are 2.14 and 2.37 Å respectively, and the distance between two Au atoms is 2.58 Å.

The corresponding Au_2 adsorption energy is 1.16 eV. Two weakly positively charged Au atoms and one Ce^{3+} were found in the charge density difference of its configuration (Figure 3b). As shown in Table 2, the Bader charges of two Au atoms are 0.07 and 0.05 respectively. Though the Bader charge of Au_2 cluster is small, it can be supported by the charge density difference findings. On the base of Bader charge and charge density difference analysis, we concluded that Au_2 cluster is oxidized and a reduced Ce^{3+} ion is formed, indicating electrons transfer from the Au_2 cluster to the substrate CeO_2.

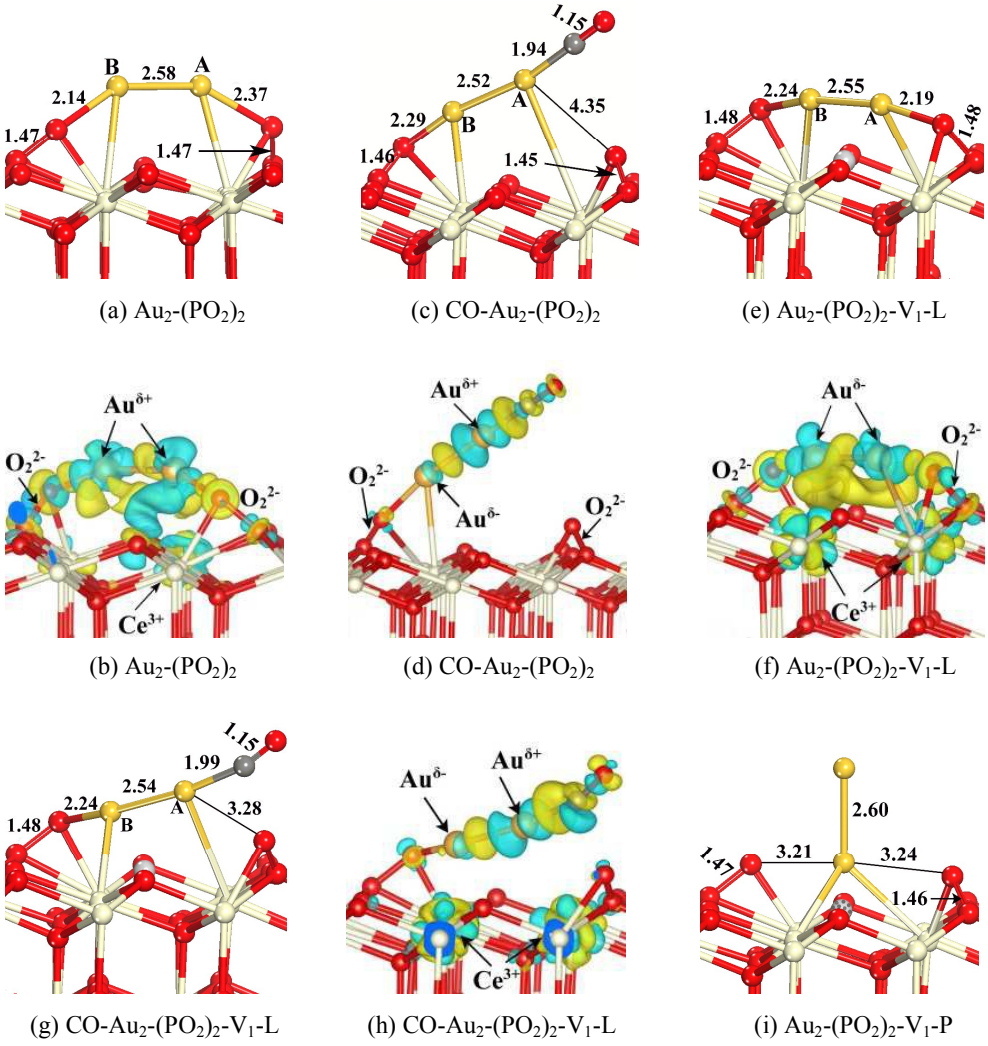

(a) Au_2-$(PO_2)_2$ (c) CO-Au_2-$(PO_2)_2$ (e) Au_2-$(PO_2)_2$-V_1-L

(b) Au_2-$(PO_2)_2$ (d) CO-Au_2-$(PO_2)_2$ (f) Au_2-$(PO_2)_2$-V_1-L

(g) CO-Au_2-$(PO_2)_2$-V_1-L (h) CO-Au_2-$(PO_2)_2$-V_1-L (i) Au_2-$(PO_2)_2$-V_1-P

Figure 3. Optimized structures of (a, e, i) Au_2 clusters on the CeO_2(111) facet and (c, g) CO adsorbed on Au_2/CeO_2(111), and (b, d, f, h) the corresponding charge density difference. (O, Ce, Au, C atoms are denoted in red, gray, yellow and dark gray, respectively. The O vacancy is represented by balls in light gray. Main bond lengths are reported in Å. Electron accumulation and depletion are represented by yellow and blue areas, respectively. The isosurface value is set as 0.005 e/Å^3).

A CO molecule can chemically adsorb on the surface of $Au_2/CeO_2(111)$ (Au_2-$(PO_2)_2$) with adsorption energy of 1.20 eV, and its optimized structure is shown in Figure 3c. The distances between Au and $O_{peroxide}$ are changed to 2.29 and 4.35 Å, respectively. After CO adsorption on the Au_2-$(PO_2)_2$ surface, there is a strong charge rearrangement at the contacts of Au/CeO_2 and Au/CO. As shown in Figure 3d, there is no reduced Ce^{3+} on the CeO_2 (111) facet, while the electron clouds of CO and Au_A is overlapped. The Bader charge results (Table 2) show that, one Au atom (Au_A) in Au_2 cluster is +0.17e and another (Au_B far from CO) is –0.13e. And the Bader charge of CO is –0.05e. Combined with the charge density and the Bader charge results, a reasonable deduction can be proposed that a reduced Ce^{3+} ion is formed when Au_2 attached to the peroxide and the reduced Ce^{3+} ion disappear after CO adsorption, which provides a strong indication of ceria acting as an electron buffer. Here, one Au adatom donates an electron to C in CO and the second Au adatom received an electron from Ce^{3+}.

The Au_2 cluster supported on the surface of CeO_2 with an oxygen vacancy and two peroxide species, that is Au_2-$(PO_2)_2$-V, has two stable adsorption structures: Au_2 cluster is located perpendicularly (P) at the surface (Au_2-$(PO_2)_2$-V-P, Figure 3i) and Au_2 lies parallel (L) at the surface (Au_2-$(PO_2)_2$-V-L, Figure 3e). Their adsorption energies are 0.58 eV and 2.65 eV, respectively. Thus, we would not consider the perpendicular structure (Au_2-$(PO_2)_2$-V-P) in the following electronic analysis and CO oxidation.

As shown in the charge density difference of Au_2-$(PO_2)_2$-V-L in Figure 3f, the surface oxygen vacancy leads to formation of two Ce^{3+} ions. As peroxide interacted with Au_2 cluster, the O-O bond was elongated from 1.44 Å to 1.48 Å, and the electrons transfer from peroxide to gold, results in the formation of weak $Au^{\delta-}$ species. These results are agreed with Bader charge analysis (Table 2, −0.05e/−0.12e). Interestingly, this weak electronegative gold cluster can adsorb CO molecule, as shown in Figure 3g. When CO accesses to the Au_2 cluster, the distance between Au and $O_{peroxide}$ is about 2.24 Å and 3.28 Å. The CO adsorption energy is 0.51 eV. The charge density difference analysis (Figure 3h) shows that, the number of reduced Ce^{3+} is unchanged after CO

adsorption, while an $Au^{\delta+}$ and an $Au^{\delta-}$ ions was formed, and their charges are +0.10e (Au_A) and –0.16e (Au_B), as shown in the Bader charge data (Table 2). It is interesting that CO interaction is more favorable on this Au_2 with $Au^{\delta-}$ than on $Au_1^{\delta-}$. Maybe Au_3 or Au_4 with $Au^{\delta-}$ will be more active still.

3.3. Au_3 and Au_4 clusters adsorbed on CeO_2 (111) surface and CO adsorption

For Au_3 cluster supported on the reduced CeO_2 (111) (CeO_2-$(PO_2)_y$-V_m) surface, the structure of Au_3-$(PO_2)_3$-V_1 is shown in Figure 4a, and the structure of Au_3-$(PO_2)_2$-V_1 is shown in Figure S3. As shown in Figure 4a, Au_3 cluster forms a triangle figure and its center is located at the top of O vacancy, in which every Au atom is anchored by peroxide. The distance between Au and $O_{peroxide}$ are 2.09, 2.22 and 2.14 Å, respectively. The lengths of three Au-Au bonds are 2.65, 2.61, 2.74 Å. After CO adsorption on Au_3 cluster (Au_3-$(PO_2)_3$-V_1, Figure 4c), the distance of Au-$O_{peroxide}$ changed to 2.11, 2.15 and 2.97 Å. The corresponding adsorption energy is 0.80 eV. To further analyze the electronic interactions between adsorbate and the CeO_2 (111) facet, we calculated the charge density difference for the Au_3-$(PO_2)_3$-V_1 structure (Figure 4b) and CO adsorption on its surface (Figure 4d). Figure 4b shows that electrons transfer from the Au_3 cluster to a surface Ce, $Au - e \rightarrow Au^{\delta+}$, $Ce^{4+} + e \rightarrow Ce^{3+}$. Hence, there are three Ce^{3+} ions on the surface, and the positive charge of the Au atoms are obtained by computing the Bader charges to be +0.07e, +0.03e and +0.17e, respectively (Table 3). Furthermore, the Au-*d* band and the O-2*p* band of the O atom in peroxide are overlapped, and we found that part of electron transfer from Au_3 to peroxide. These results show that ceria has the capacity of storing electrons. In comparison with the adsorption of Au_1 and Au_2 on ceria, for the adsorption of Au_3, the ability of ceria storing electrons is better to prevent formation of negatively charged adsorbed Au_3, to help its reaction with CO. After CO adsorption, the number of Ce^{3+} ion is unchanged, and the charges of Au atoms are changed to +0.23e, +0.05e and +0.09e (Table 3) respectively. This shows that, after CO adsorption, the charge redistribution occurred in the Au/CeO_2 and CO/Au interfaces, where the electrons transferred from peroxide (close to CO) feedback to Au_3, and from Au_3 cluster to CO.

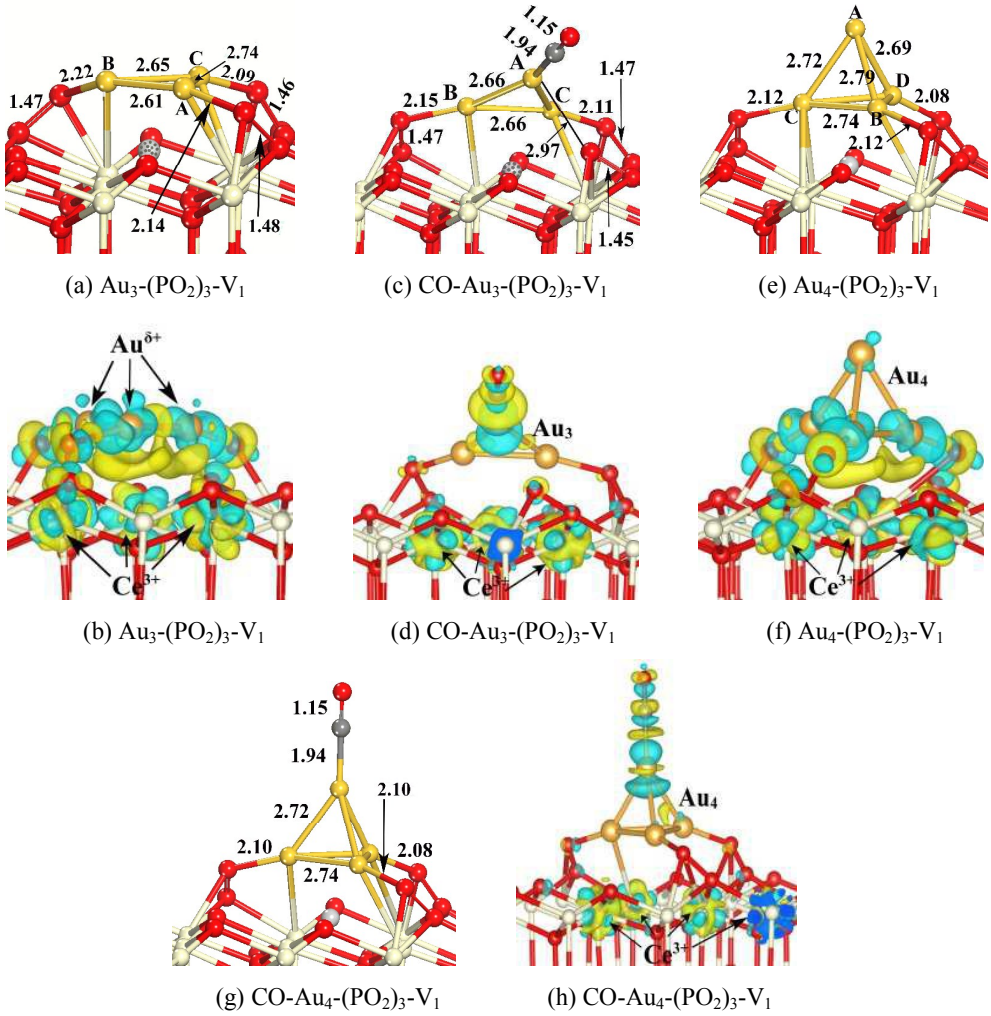

Figure 4. Optimized structures of (a) Au_3 and (e) Au_4 clusters on the $CeO_2(111)$ facet and CO adsorption on (c) $Au_3/CeO_2(111)$ and (g) $Au_4/CeO_2(111)$, and (b, d, f, h) the corresponding charge density difference. (O, Ce, Au, C atoms are denoted in red, gray, yellow and dark gray, respectively. The O vacancy is represented by balls in light gray. Main bond lengths (Å) are reported. Electron accumulation and depletion are represented by yellow and blue areas, respectively. The isosurface value is set as 0.005 e/Å^3).

For Au_4 clusters supported on reduced CeO_2 (111) facet, that is Au_4-$(PO_2)_3$-V_1, its configurations are shown in Figure 4e, and the configurations of Au_4-$(PO_2)_4$-V_2 are shown in Figure S3c. The results show that, Au_4 cluster forms a pyramidal structure, and is located at the top site of the surface oxygen vacancy, in which its adsorption energy is 2.84 eV (Table 3). After CO adsorbed on Au_4/CeO_2 ($(PO_2)_3$-V_1) (Figure 4g), the bond lengths of C-O and Au-C in the CO adsorption structure are ~1.15 and 1.94 Å respectively, and its adsorption energy was calculated to be 1.44 eV. The charge density difference analysis of Au_4-$(PO_2)_3$-V_1 (Figure 4f) shows that, each

of peroxide interacts with one Au atom in the bottom layer, resulting in the electrons transfer from peroxide O-2*p* states to Au-*d* states. In addition, the electrons of Au atoms transferred to the substrate, three reduced Ce^{3+} ions existed on the Au_4-$(PO_2)_3$-V_1 surface, and the charges of Au atoms were estimated by Bader charge to be –0.09e, +0.08e, +0.09e and +0.21e, respectively (Table 3).

As shown in Figure 4g, CO is attached to Au_A (-0.09e/slight electronegative, Table 3). However, $Au^{\delta-}$ ion is inactive for CO adsorption, and the electrons of Au atoms through peroxide transferred to substrate Ce, the number of the partially reduced Ce^{4+} ions is up to four (Figure 4h). At the same time, CO also gets ~0.06e from Au. The lengths of Au-$O_{peroxide}$ bonds are unchanged. The Bader charges of Au atoms are calculated to be +0.26e, +0.08e, +0.07e and +0.10e, respectively, which is well consistent with the results of charge density difference (Figure 4h).

For Au_4-$(PO_2)_4$-V_2 configuration (Figure S3c), all Au atoms lie on the surface with two structures of Au_2-$(PO_2)_2$-V_1-L. The Au_4 adsorption energy is 5.00 eV. CO can chemically adsorb on the supported Au_4 (Au_4-$(PO_2)_4$-V_2) with the adsorption energy of 0.57 eV.

The research results for Au_3 and Au_4 clusters further validate that, CeO_2 structures containing both peroxide and vacancy (CeO_2-$(PO_2)_y$-V_m) help Au cluster adsorption/attachment on CeO_2(111) facet. With increasing Au atoms in the Au clusters over CeO_2-$(PO_2)_y$-V_m, CO adsorption on this surface would be stronger than Au_1 and Au_2, in which CeO_2 acted as the electron buffer during both Au adsorption on CeO_2 and CO adsorption on Au_x/CeO_2.

Table 3. The Au_3 and Au_4 clusters or CO adsorption (eV) and the Bader charge

	E_{ad} /eV	Au—Bader charge /e				CO-Bader charge/e
		Au_A	Au_B	Au_C	Au_D	
Au_3-$(PO_2)_3$-V_1	3.94	+0.07	+0.03	+0.17		
CO-Au_3-$(PO_2)_3$-V_1	0.80	+0.23	+0.05	+0.09		-0.04
Au_4-$(PO_2)_3$-V_1	2.84	-0.09	+0.08	+0.09	+0.21	
CO-Au_4-$(PO_2)_3$-V_1	1.44	+0.26	+0.08	+0.07	+0.10	-0.06

3.4. Density of States.

The typical density of states (DOS) for Au_1-$(PO_2)_1$ and CO adsorbed on Au_1-$(PO_2)_1$ configurations are shown in Figure 5. Comparing with the DOS of the PO_2 and Au-PO_2, we found that two new features (labeled "A" and "B") appeared in the Au-PO_2 structure. For the Au-PO_2 structure, the filled Ce-4*f* band appearred between -1 and 0 eV (the A feature), which reveals that one Ce^{4+} is reduced to Ce^{3+} ion. Obviously, the electron transfer from Au to ceria through the Au-$O_{lattice}$ bond. Therefore, the overlapping between Au and $O_{lattice}$ gives rise to the C peak at -6 ~ -5 eV. The feature B is related to the Au-$O_{peroxide}$ bonding at -8 ~ -7 eV, reveals that the Au-$O_{peroxide}$ bond results mostly from the overlap of Au-*d* states and the O-*p* states in peroxide. Based on the analysis of charge density difference, this is due to electron of Au transfer to O. After CO adsorption, the distance between Au and $O_{peroxide}$ is extended to 3.06Å (Figure 2c), indicating there is few interaction between them. And the charge of $Au^{\delta+}$ transfered C atom and fed back to peroxide at the CO/Au and Au/CeO_2 interfaces or contacts, respectively. The overlapping of Au-*d* states and the C-*p* states results in the D feature at -11 ~ 7 eV in Figure 5B.

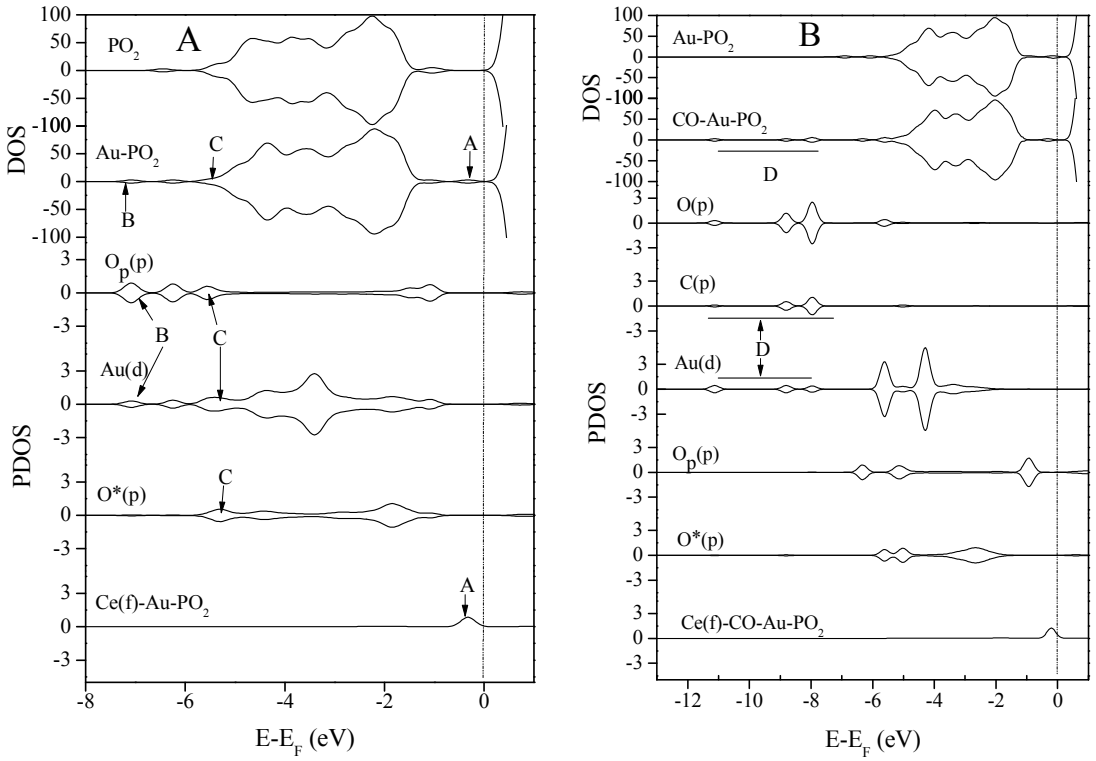

Figure 5. Density of states of Au_1-$(PO_2)_1$ and CO-Au_1-$(PO_2)_1$ and the projected DOS analysis. The vertical dashed line indicates the Fermi level at 0 eV. (O − O atom in CO; O_p − O atom in peroxide; O* − lattice O).

On the basis of DOS, we can see, when Au supported on CeO_2-$(PO_2)_1$ surface, charge would transfer in the following order: $PO_2 \rightarrow Au \rightarrow O_{lattice} \rightarrow Ce^{4+}$, $Ce^{4+} + Au^0 \rightarrow Ce^{3+} + Au^{\delta+}$, in which CeO_2 acts as electronic buffer.

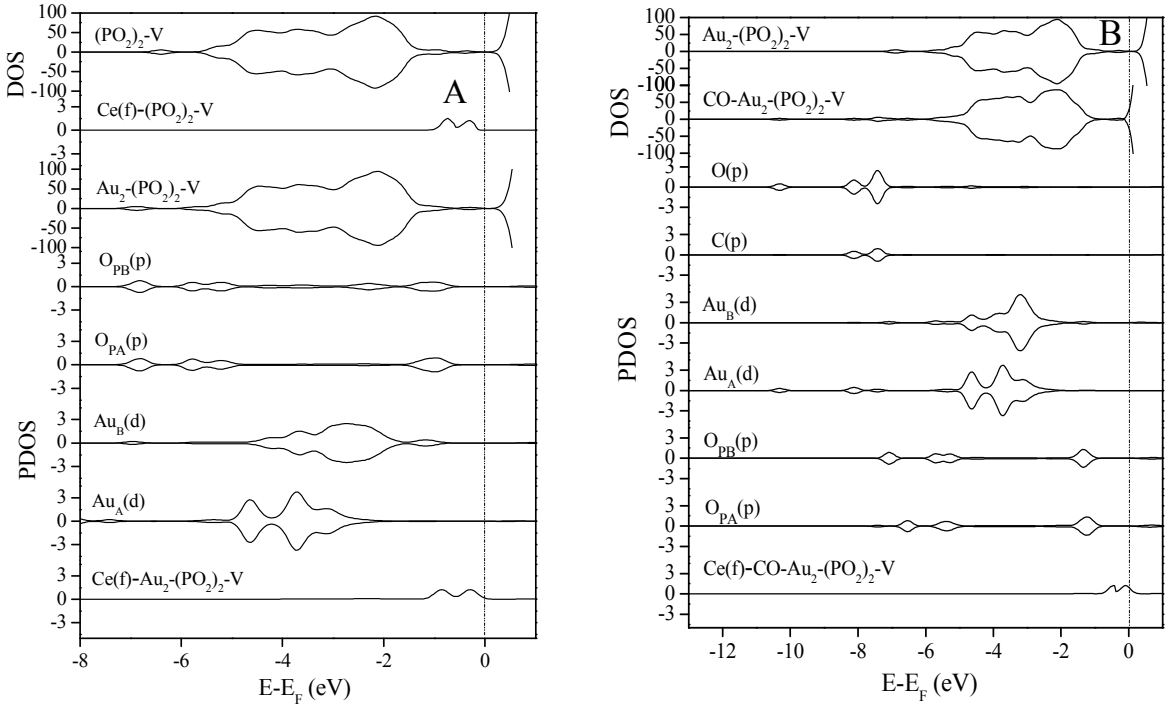

Figure 6. Density of states of Au_2-$(PO_2)_2$-V_1-L and CO-Au_2-$(PO_2)_2$-V_1-L and the projected DOS analysis. The vertical dashed line indicates the Fermi level at 0 eV. (O − O atom in CO; O_p − O atom in peroxide; In Au_2-$(PO_2)_2$-V_1-L and CO-Au_2-$(PO_2)_2$-V_1-L configurations, Au_A connected to O_{PA} and Au_B connected to O_{PB}).

The DOS for Au_2-$(PO_2)_2$-V_1-L and CO-Au_2-$(PO_2)_2$-V_1-L was shown in Figure 6. In Ce PDOS of $(PO_2)_2$-V, Au_2-$(PO_2)_2$-V and CO-Au_2-$(PO_2)_2$-V, two Ce^{3+} ions were formed and partially occupied electronic DOS peaks appeared at -2 ~ 0 eV. And the number of Ce^{3+} ions is unchanged during Au_2 or CO adsorption. No electron transfer between gold and Ce^{3+}/Ce^{4+} ion. In Comparison with $O_{peroxide}$ and Au PDOS of $(PO_2)_2$-V and Au_2-$(PO_2)_2$-V, the peaks of the similar B feature in Figure 5A appear at -8 ~ -6 eV, which indicates that the overlap between $O_{peroxide}$ and Au. Based on the analysis of charge density difference and Bader charge, this is due to a few electron of peroxide transfer to Au atom. As shown in Figure 6B, when CO attached on Au_A, the B peak reduced greatly at -8 ~ -6 eV, while the new peak appeared around -10 eV, which results from the overlap of Au_A-*d* states and the C-*p* states. In addition, the *d* orbitals of the two Au atoms are overlapped at

-6 ~ -2 eV, which shows that the electrons transfer from Au_A to Au_B.

The DOS analysis show that charge transfers from peroxide to Au when Au_2 adsorbed on $(PO_2)_2$-V_1-L surface, and Au-*d* states and $O_{peroxide}$-*p* states are overlapped. After CO adsorption, electrons feed from Au_A to peroxide, by the help of the bond of Au_A and CO. So peroxide is an important species in Au_2 or CO adsorption.

3.5. Effect of peroxide on reduced CeO_2 (111) facet

Experimentally, using Raman spectroscopy, peroxide and superoxide species were characterized on Au/CeO_2 surface,[23] and it was found a correlation between the catalytic activity of gold and peroxide and superoxide species. The formation of reactive oxygen species on the nanocrystalline support is enhanced by the gold.[32] Therefore, we studied Au adsorption around peroxide. We simulated a structure, in which the boundary of Au cluster is archored by peroxide, rather than each Au atom was archored, in which only the boundary Au is active and other gold atom is inert.

Au supported on ceria surface can be described as Scheme 1. Oxygen vacancy is the common defect for most metal oxides. On ceria surface containing the O vacancies, supported Au atom will become negatively charged.[24,28] And $Au^{\delta-}$ ions are inactive for CO oxidation. Herein, our results show that O_2 adsorbed on reduced CeO_{2-x}(111) facet (formed peroxide) can transfer the charge from $Au^{\delta-}$ ions to peroxide. The negative charge of Au_x cluster adsorbed on the CeO_2-$(PO_2)_y$-V_m surface is lower than that on CeO_2 with only oxygen vacancy, in which electrons transfer from Au atom to peroxide. The charges of Au_x ($x > 1$) on the CeO_2-$(PO_2)_y$-V_m surface are close to either slight negatively charged or even slight positively charged, which promotes CO adsorption on the Au_x/CeO_2 surface. When x=1 (Au_1), the distance between Au atom and $O_{peroxide}$ is 3.51 Å, no electron transfers from Au atom to peroxide.

On the basis of the charge density difference and the Bader charge analyses and the results mentioned-above, we can find, ceria has the strong capability of electron storage. For example, when Au supported on the upper site of O vacancy on the CeO_2 surface (Figure 1f), CeO_2 will transfer removable electron to Au ($Ce^{3+} + Au^0 \rightarrow Ce^{4+} + Au^{\delta-}$). While Au_x cluster ($x \geq 3$)

supported on the surface of CeO_2 with peroxide and O vacancy, Au will transfer electron to CeO_2 substrate: $Ce^{4+} + Au^0 \rightarrow Ce^{3+} + Au^{\delta+}$. In a word, CeO_2 acts as electronic buffer.

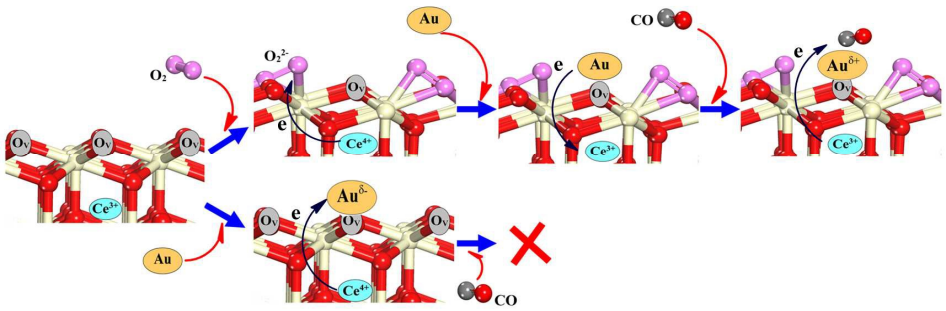

Scheme 1. Configurations of Au supported on CeO_2 with O vacancy or both peroxide and O vacancy, and CO adsorbed on Au/CeO_2.

4. Conclusions

In summary, by means of DFT+U calculations, we studied the adsorption behaviors of Au_x(x=1-4) clusters on the various CeO_2(111) facets containing oxygen vacancies, peroxide and superoxide species. It has been found that, when Au_1 supported on the CeO_2 (111) facet with an O vacancy to form a strong negatively charged $Au^{\delta-}$, which is not favorable for CO adsorption on its surface; the structure of CeO_2(111) containing both O vacancy and peroxide is stable and can effectively support Au cluster (Au_x-$(PO_2)_y$-V_m), which enables Au perfectly supporting on the CeO_2 (111) facet to overcome Au-Au bond reunion.

On the basis of the charge density difference and Bader charge analyses, we further revealed the electron transfer mechanism. When Au_2 supported on CeO_2 with two peroxides and only O vacancy (Au_2-$(PO_2)_2$-V_1), Au_2 adsorbed strongly and parallel on the CeO_2-$(PO_2)_2$-V_1, in which the electrons transfer from peroxide to the supported Au atom to form weak $Au^{\delta-}$. However, this weak negatively charged gold cluster can adsorb CO molecule. When Au_x cluster ($x \geq 3$) supported on the surface of CeO_2 with peroxide and O vacancy, Au will transfer electron to CeO_2 substrate. With increasing Au atoms in the Au clusters over CeO_2-$(PO_2)_y$-V_m, CO adsorption on this surface would be stronger. During both Au supported on CeO_2 and CO adsorbed on Au_x/CeO_2, CeO_2 acts as the electron buffer. The CeO_2 structures containing both peroxide and vacancy

(CeO_2-$(PO_2)_y$-V_m) help Au cluster adsorption/attachment on the CeO_2(111) facet, and CO adsorption was greatly improved, which will set a basic foundation for the next step: CO oxidation. Detailed findings will release later.

Electronic Supplementary Information (ESI) available:

Structures and charge density differences for CeO2 (111) facet containing single O vacancy (Figures S1), peroxide, superoxide, and both peroxide and O vacancy (Figure S2), and structures of Au_3-$(PO_2)_2$-V_1 and Au_4-$(PO_2)_4$-V_2 and CO oxidation on them (Figure S3). See DOI: 10.1039/b000000x/

Acknowledgements

This project was financially supported by the National Natural Science Foundation of China (21273150, 21203119), the National Basic Research Program of China (2013CB933201), the national high technology research and development program of China (2011AA03A406, 2012AA062703), the Shanghai Natural Science Foundation (12ZR1430800), and the Shanghai Innovation Program (12YZ161).

Notes and References

1. P. Ghosh, M. F. Camellone and S. Fabris, J. Phys. Chem. Lett., 2013, 4, 2256.
2. F. Chen, D. Liu, J. Zhang, P. Hu, X.-Q. Gong and G. Lu, Phys. Chem. Chem. Phys., 2012, 14, 16573.
3. C. Liu, Y. Tan, S. Lin, H. Li, X. Wu, L. Li and Y. Pei, J. Am. Chem. Soc., 2013, 135, 2583.
4. F. Chen, J. Cheng, P. Hu and H. Wang, Surf. Sci., 2008, 602, 2828.
5. S. Zhang, X. -S. Li, B. Chen, X. Zhu, C. Shi and A. -M. Zhu, ACS Catal., 2014, 4, 3481.
6. Z. P. Liu, S. J. Jenkins and D. A. King, Phys. Rev. Lett., 2005, 94, 196102.
7. F. Vindigin, M. Manzoli, T. Tabakova, V. Idakiev, F. Boccuzzi and A. Chiorino, Phys. Chem. Chem. Phys., 2013, 15, 13400.
8. A. B. Vidal, L. Feria, J. Evans, Y. Takahashi, P. Liu, K. Nakamura, F. Illas and J. A. Rodriguez, J. Phys. Chem. Lett., 2012, 3, 2275.
9. C. Hamill, R. Burch, A. Goguet, D. Rooney, H. Driss, L. Petrov and M. Daous, Appl. Catal. B: Environ., 2014, 147, 864.
10. T. D. Chau, T. Visart de Bocarme and N. Kruse, Catal. Lett. 2004, 98, 85.

11. C. P. Vinod, J. W. Niemantsverdriet Hans and B. E. Nieuwenhuys, Appl. Catal. A: Gen., 2005, 291: 93.
12. J. Zhang, X. Q. Gong and G. Z. Lu, Chinese J. Catal., 2014, 35, 1305.
13. G. Pattrick, E. van der Lingen, C. W. Corti, R. J. Holliday and D. T. Thompson, Top. Catal., 2004, 30-31, 273.
14. M. Haruta, T. Kobayashi, H. Sano and N. Yamada, Chem. Lett., 1987, 16, 405.
15. M. Haruta, S. Tsubota, T. Kobayashi, H. Kageyama, M. J. Genet and B. Delmon, J. Catal. 1993, 144, 175.
16. M. Valden, X. Lai and D. W. Goodman, Science, 1998, 281, 1647.
17. R. Meyer, C. Lemire, S. K. Shaikhutdinov and H. Freund, Gold Bull, 2004, 37, 72.
18. M. Haruta, Faraday Discuss., 2011, 152, 11.
19. N. Ta, F. Wang, H. Li and W. Shen, Catal. Today, 2011, 175(1): 541.
20. N. Ta, J. Liu, S. Chenna, P. A. Crozier, Y. Li, A. Chen and W. Shen, J. Am. Chem. Soc., 2012, 134, 20585.
21. S. Chen, L. Luo, Z. Jiang and W. Huang, ACS Catal. , 2015, 5, 1653.
22. P. Concepción, S. Carrettin and A. Corma, Appl. Catal. A: Gen., 2006, 307, 42.
23. J. Guzman, S. Carrettin and A. Corma, J. Am. Chem. Soc, 2005, 127, 3286.
24. M. F. Camellone and S. Fabris, J. Am. Chem. Soc., 2009, 131, 10473.
25. A. M. Venezia, P. Giuseppe, A. Longo, G. Di Carlo, M. P. Casaletto, F. L. Liotta and G. Deganello, J. Phys. Chem. B, 2005, 109, 2821.
26. C. Zhang, A. Michaelides, D. A. King and S. J. Jenkins, J. Phys. Chem. C, 2009, 113, 6411.
27. N. C. Hernández, R. Grau-Crespo, N. H. de Leeuw and J. F. Sanz, Phys. Chem. Chem. Phys., 2009, 11, 5246.
28. T. Tabakova, F. Boccuzzi, A. Chiorino, M. Manzoli and D. Andreeva, Appl. Catal. A: Gen., 2003, 252, 385.
29. S. Carrettin, P. Concepción, A. Corma, J. M. López Nieto and V. F. Puntes, Angew. Chem., Int. Ed., 2004, 43, 2538.
30. X. -S. Huang, H. Sun, L.-C. Wang, Y.-M. Liu, K. –N. Fan and Y. Cao, Appl. Catal. B: Environ., 2009, 90, 224.
31. C. Pan, D. Zhang, L. Shi and J. Fang, Eur. J. Inorg. Chem., 2008, 2008: 2429.
32. J. Guzman, S. Carrettin, J. C. Fierro-Gonzalez, Y. Hao, B. C. Gates and A. Corma, Angew. Chem., Int. Ed., 2005, 44, 4778.
33. A. Martínez-Arias, J. Conesa and J. Soria, Res. Chem. Intermed., 2007, 33, 775.
34. C. Li, K. Domen, K.-I. Maruya and T. Onishi, J. Catal., 1990, 123, 436.
35. Y. M. Choi, H. Abernathy, H.-T. Chen, M. C. Lin and M. Liu, ChemPhysChem, 2006, 7 (9), 1957.
36. V. V. Pushkarev, V. I. Kovalchuk and J. L. d'Itri, J. Phys. Chem. B, 2004, 108, 5341.
37. Z. Wu, M. Li, J. Howe, H. M. Meyer and S. H. Overbury, Langmuir, 2010, 26, 16595.
38. H.-Y. Li, H.-F. Wang, X.-Q. Gong, Y.-L. Guo, Y. Guo, G. Lu and P. Hu, Phys. Rev. B., 2009, 79 (19), 193401.
39. M. Huang and S. Fabris, Phys. Rev. B, 2007, 75 (8), 081404.
40. Y. Zhao, B.-T. Teng, X.-D. Wen, Y. Zhao, Q.-P. Chen, L.-H. Zhao and M.-F. Luo, J. Phys. Chem. C, 2012, 116, 15986.
41. W. J. Zhu, J. Zhang, X. Q. Gong and G. Z. Lu, Catal. Today 2011, 165 (1), 19.

42. H. Y. Kim and G. Henkelman, J. Phys. Chem. Lett., 2012, 3, 2194.
43. H. Y. Kim, H. M. Lee and G. Henkelman, J. Am. Chem. Soc., 2012, 134, 1560.
44. H.-F. Wang, X.-Q. Gong, Y.-L. Guo, Y. Guo, G. Z. Lu and P. Hu, J. Phys. Chem. C, 2009, 113, 10229.
45. Z. Yang, T. K. Woo and K. Hermansson, J. Chem. Phys., 2006, 124, 224704.
46. W. Song, E. J. M. Hensen, ACS Catal., 2014, 4, 1885.
47. S. M. Kozlov and K. M. Neyman, Phys. Chem. Chem. Phys., 2014, 16, 7823.
48. W. Cen, Y. Liu, Z. Wu, H. Wang and X. Weng, Phys. Chem. Chem. Phys., 2012, 111, 1.
49. M. M. Branda, N. C. Hernández, J. F. Sanz and F. Illas, J. Phys. Chem. C, 2010, 114, 1934.
50. M. M. Branda, R. M. Ferullo, M. Causá and F. Illas, J. Phys. Chem. C, 2011, 115, 3716.
51. M. M. Branda, C. Loschen, K. M. Ney man and F. Illas, J. Phys. Chem. C, 2008, 112, 17643.
52. G. Kresse and J. Hafner, Phys. Rev. B, 1994, 49, 14251.
53. G. Kresse and J. Furthmuller, Phys. Rev. B, 1996, 54, 11169.
54. G. Kresse and D. Jouber, Phys. Rev. B, 1999, 59, 1758.
55. O. Bengone, M. Alouani, P. Blochl and J. Hugel, Phys. Rev. B, 2000, 62, 16392.
56. S. Fabris, S. de Gironcoli, S. Baroni, G. Vicario and G. Balducci, Phys. Rev. B, 2005, 71, 041102.
57. M. Nolan, S. Grigoleit, S. C. Parker and G. W. Watson, Surf. Sci., 2005, 576, 217.
58. M. Nolan, S. C. Parker and G. W. Watson, Surf. Sci., 2005, 595, 223.
59. M. Nolan, S. C. Parker and G. W. Watson, J. Phys. Chem. B, 2006,110, 2256.
60. C. Zhang, A. Michaelides, D. A. King and J. J. Stephen, J. Chem. Phys., 2008, 129(19): 194708.
61. C. Zhang, A. Michaelides, D. A. King and J. J. Stephen, J. Am. Chem. Soc., 2010, 132(7): 2175.
62. Z. K. Han and Y. Gao, Nanoscale, 2015, 7(1): 308.
63. W. Song and E. J. M. Hensen, J. Phys. Chem. C, 2013, 117(15): 7721.
64. N. J. Castellani, M. M. Branda and K. M. Neyman, J. Phys. Chem. C, 2009, 113(12): 4948.
65. L. Cui, Y. Tang, H. Zhang, L. G. Hector Jr., C. Ouyang, S. Shi, H. Li and L. Chen, Phys. Chem. Chem. Phys., 2012, 14, 1923.
66. Y. Chen, P. Hu, M.-H. Lee and H. Wang, Surf. Sci., 2008, 602, 1736.
67. B. Teng, F. Wu, W. Huang, X. Wen, L. Zhao and M. Luo, ChemPhysChem, 2012, 13, 1261.
68. F. Esch, S. Fabris, L. Zhou, T. Montini, C. Africh, P. Fornasiero, G. Comelli and R. Rosei, Science, 2005, 309: 752.
69. C. Zhang, A. Michaelides, D. A. King and S. J. Jenkins, Phys. Rev. B, 2009, 79, 075433.